



# Time-series analysis of Sentinel-2 satellite images for sunflower yield estimation

Khilola Amankulova<sup>a,\*</sup>, Nizom Farmonov<sup>a</sup>, László Mucsi<sup>b</sup>

<sup>a</sup> Doctoral School of Geosciences, Department of Geoinformatics, Physical and Environmental Geography, University of Szeged, Egyetem utca 2, Szeged 6722, Hungary

<sup>b</sup> Department of Geoinformatics, Physical and Environmental Geography, University of Szeged, Egyetem utca 2, Szeged 6722, Hungary

## ARTICLE INFO

### Keywords:

Remote sensing  
Random forest regression  
Sentinel-2  
Sunflower  
Yield prediction

## ABSTRACT

Accurate estimates and predictions of sunflower crop yields at the pixel and field level are critically important for farmers, service dealers, and policymakers. Several models based on remote sensing data have been developed in yield assessment, but their robustness—especially in small field scale areas—needs to be examined. Here we aim to develop a robust methodology for estimation/prediction of sunflower yield at pilot field scale using Sentinel-2 remote sensing satellite imagery. We conducted the study in Mezöhegyes, south-eastern Hungary. The Random Forest Regression (RFR), a machine learning technique was used in this research to translate the Sentinel-2 spectral bands to sunflower yield based on crop yield data provided by a combine harvester equipped with a yield-monitoring system. Sentinel-2 images obtained from April to September were used to find the best image for prediction. The satellite image acquired on June 28 was found best and considered further for prediction sunflower yield. A developed training model was tested and validated in 10 different parcels to evaluate the performance of the prediction. We examined the results of the prediction model (predicted) against the actual yield data (observed) collected by a combine harvester. The results demonstrated that using 10 spectral bands from Sentinel-2 imagery the best time to predict sunflower yields was between 85 and 105 d into the growing season during the flowering stage. This model achieved high accuracy with low normalized root means square error (RMSE) ranging from 121.9 to 284.5 kg/ha for different test fields. Our results are promising because they prove the possibility of predicting sunflower grain yield at the pixel or field level, 3–4 months before the harvest, which is crucial for planning food policy.

## 1. Introduction

Sustainable agricultural crop production is essential to the provision of food grain products, but various obstacles prevent farmers from achieving the potential high crop yield from cultivated arable lands [1]. Early-stage crop growth and crop yield information is necessary for synchronizing agricultural production to meet national and global food demands and maintain food security [2]. Sunflower is an essential oilseed plant that originates from South America and is currently cultivated in many countries in the world [3]. Total annual production is over 50 million tonnes and has been increasing over the past decade [4, 5]. Sunflower ranks second most consumed oil crop after soybean due to its very high oil content (36–55%). Besides, oil extracted from sunflower

oilseeds has been considered healthy and nutritional food that is beneficial for human consumption. Moreover, the pharmacological survey on sunflower showed that it has many medicinal values to protect from different kinds of illnesses. The advantages of sunflower such as blood pressure and diabetic control, skin protection, and lowering cholesterol and other functions. Hungary is one of the larger sunflower producer in the European Union member states. Hungary accounted for nearly 20% of the EU's total production (8.8 million tonnes) which makes it the second larger sunflower producer country after Romania in 2020, according to the EUROSTAT. There is high demand to expand the cultivated lands and increase sunflower seed production in the country.

Considering the limited availability of arable lands, a significant part of this increased demand will be met through intensive precision

*Abbreviation:* ESA, European Space Agency; EVI, enhanced vegetation index; GCOS, global climate observing; GIS, geographic information systems; GPS, global positioning systems; IoT, internet of things; LAI, leaf area index; LSWI, land surface water index; ML, machine learning; MLR, multiple linear regression; MODIS, moderate resolution imaging spectroradiometer; NDVI, normalized difference vegetation index; NDWI, normalized difference water index.

\* Corresponding author.

E-mail address: [amankulova.khilola@stud.u-szeged.hu](mailto:amankulova.khilola@stud.u-szeged.hu) (K. Amankulova).

<https://doi.org/10.1016/j.atech.2022.100098>

Received 11 June 2022; Received in revised form 18 July 2022; Accepted 25 July 2022

Available online 27 July 2022

2772-3755/© 2022 The Author(s). Published by Elsevier B.V. This is an open access article under the CC BY license (<http://creativecommons.org/licenses/by/4.0/>).

agriculture, with a concomitant increased use of fertilizers, pesticides, water, and other inputs [6]. Fertilizers and chemicals for agricultural production cause yield reduction and increased water and nutrient losses from agriculture that lead to environmental degradation and eutrophication [7–9]. There are several ways of predicting crop yields, from a field to regional scale using remote sensing techniques [10]. Advanced technologies such as remote sensing, global positioning systems (GPS), geographic information systems (GIS), the internet of things (IoT), big data analysis, and artificial intelligence (AI) and machine learning (ML) are important tools for optimizing agricultural practices, enhancing production, and reducing inputs and crop yield losses [11–13]. AI methods, such as ML algorithms (for instance, artificial neural networks) have been used to estimate ET, soil moisture, and crop behaviour predictions for automated and precise application of water, fertilizer, herbicides, and insecticides [14]. These breakthrough technologies and tools provide timely information to farmers to characterize spatial variability (for instance, of soils) within farms and large crop fields that negatively affect crop growth and yields [15]. Remote sensing can be used to evaluate spatial variability in crop yield [16], and can be an efficient technology in precision agriculture for estimating crop status during the growing season, particularly in assessing the correlation between spectral vegetation indices during crop growth and crop yield [17]. Estimating crop yields at the field level before harvesting is of great interest to farmers, government agencies, traders, decision makers, and policymakers. Meanwhile, early prediction of yields informs decisions on the collection, processing, storage, transportation, and export and import of agricultural products [18].

The many earth observation systems that have been developed include the moderate resolution imaging spectroradiometer (MODIS) and Landsat satellite imagery, which is commonly used for Agricultural applications [19]. The Sentinel-2 satellite developed by the European Space Agency (ESA) as part of the Copernicus program in 2015 carries a multispectral high-resolution instrument (MSI), which has great potential to monitor crop plants at farm scale over agricultural lands [20].

Several approaches have been developed to forecast different crop yields at regional and field scale, based on remotely sensed vegetation indices and crop yield data [21–26]. Narin and Abdikan et al. [27] estimated sunflower yield using crop phenological stages obtained from Sentinel-2 satellite images based on linear regression. The study was carried out in Zile district of Tokat province, Turkey which has dense sunflower production. In their research, ten Vegetation Indices (VIs) were used from Sentinel-2 data acquired during the growing phases of sunflowers. As a result of the study,  $R^2 = 0.67$  the highest coefficient of determination and The Root Mean Square Error (RMSE) lower than 13 kg/da was found on 30 June, at the stage of inflorescence emergence. The best forecast was obtained by NDVI ( $R^2=0.74$  and  $RMSE=10.80$  kg/da) about three months before the harvesting stage. Fieuzal et al. [28] predicted sunflower seed by assimilating ground and optical or microwave satellite data into an agrometeorological model at the field scale using the leaf area index (LAI) and/or the dry mass (DM) of the crop. They used an agrometeorological model called SAFY-WB which combines crop growth and a water balance e (FAO-56) model. The LAI was extracted from multitemporal satellite images obtained by five sensors both Synthetic Aperture Radar (SAR) and optical (TerraSAR-X, Radarsat-2, Formosat-2, Spot-4/5), over the study area located in southwestern France whereas DM was measured during the field campaign. Firstly, they simulated temporal dynamics of biophysical parameters (i.e., LAI, DM, and yield) and calibrated with measured biophysical parameters. The result demonstrated that temporal changes of LAI and DM can be accurately calibrated over the five studied working farms with  $R^2_{DM} > 0.85$  and  $R^2_{LAI} > 0.94$  with a relative root-mean-square error (RMSE)  $< 30\%$ . Then, sunflower yield was estimated ( $R^2 > 0.85$ ) over 140 ha, with RMSE ranging from 0.20 to 0.54 t/ha by using both the LAI derived from radar and optical data. Trépos et al. [25] predicted sunflower crop yield using model SUNFLO (combine of the simulation of the crop model and the time series of the

leaf area index (LAI) derived from Sentinel-2A and Landsat-8 and extracted over 281 fields near Toulouse, France). They proved that data assimilation leads to statistically significant improvement in predictions than the simulation alone achieves (from an RMSE of 9.88 q/ha to an RMSE of 7.49 q/ha). Their model obtained better results by relying on smoothed LAI rather than raw LAI.

The main purpose of this study is to develop a robust method to estimate and predict sunflower crop yield by maximizing the high spatial resolution of Sentinel-2 satellite imagery, at the field level scale of agricultural fields by using RFR. We hypothesized that the yield data would have a significant correlation with Sentinel-2 spectral reflectance values. We addressed the following relationships in this research:

- 1 the connection Sentinel-2 derived spectral information and sunflower crop yield data;
- 2 the optimal correlation model between 10 spectral bands and crop yield data using RFR to estimate sunflower crop yield before the harvesting stage.

In addition, we assessed the significant differences between observed and predicted yield values in different yield months. We were thus able to determine both the accuracy of the overall prediction and the prediction model that gave the best result.

## 2. Material and methods

### 2.1. Study area

The experimental farm of Mezőhegyes is located in Mezőhegyes town, Békés and Csongrád-Csanád counties, Hungary, next to the Romanian border (latitude  $46^\circ 19' N$ , longitude  $20^\circ 49' E$ ) (Fig. 1). The total administrative area of the town is 15 544 hectares, and its population is 4950 people. Chernozem is a very common type of soil that supports both plant growth and high yields [29]. The meadow and lowland chernozem, with their high lime content, provides an excellent basis for field plant cultivation. Chernozem is a very fertile soil that produces high agricultural yields and offers excellent agronomic conditions to produce crops, especially cereals and oilseeds. Mezőhegyesi Ménesbirtok Zrt. (the experimental farm of Mezőhegyes) plays an important role in the lives of both Mezőhegyes and the neighbouring settlements. According to the operational water scarcity assessment and forecasting system in Hungary and the experimental farm of Mezőhegyes, between May 21 and June 28, 2020, a very high rainfall for this agricultural area was recorded at 190.6 mm. Climate records at Mezőhegyes station (next to the selected fields) show that annual rainfall there was 575 mm (458 mm in-crop) for 2020 season (Fig. 2).

### 2.2. Field data collection and preparation

#### 2.2.1. Crop information

The sunflower is one of the common crop species in the Mezőhegyes. The total area of arable land is 8126 hectares, and includes 102 field plots of different sizes. Field preparation was carried out for the seeding process on March 26 and sunflowers were sown on March 31, 2020. There were 20 parcels occupied by sunflowers totalling 1174,4 hectares, which in 2020 contributed almost 15% of the total area. Farmers implemented weed control on May 7 using chemicals against weeds followed by those against insects and bacteria, conducted on June 29. We administered no additional nutrients or irrigation to increase the fertility of the sunflowers during the growing season, and on October 28, at the end of the growing season, crop harvested with a John Deere W650i combine harvester equipped with a yield-mapping system providing, through the associated Green Star software, a yield data in a point shape format approximately one yield record every 2 seconds that were viewed and manipulated in a geographic information system (GIS). Because, as chemicals to speed up the ripening of the sunflower seeds



Fig. 1. Study area. The areas highlighted with red colour indicate test fields. (Natural colour composite from Sentinel-2 imagery; bands: RGB (4, 3, 2); acquisition date: 28th June 2020)

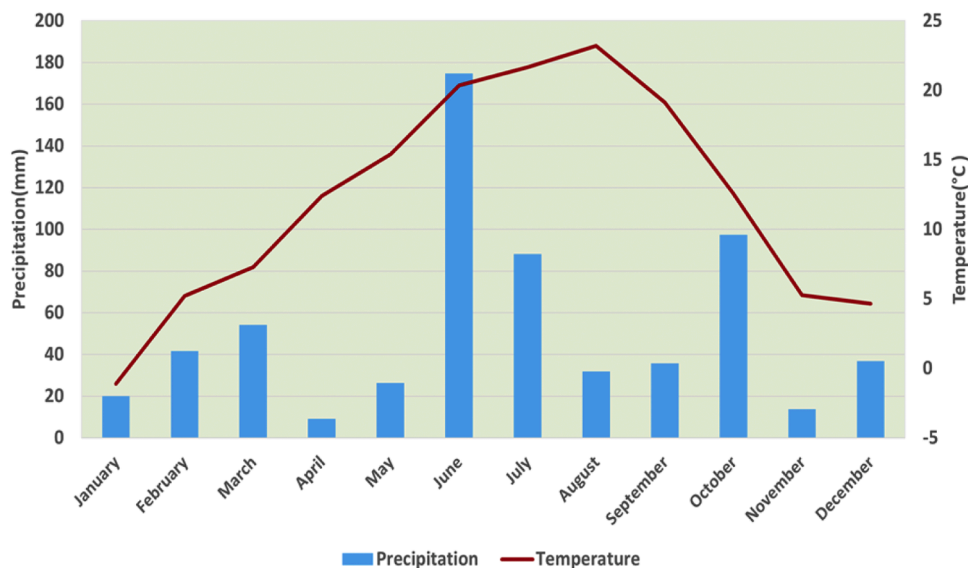


Fig. 2. Monthly precipitation and temperature at: Mezöhegyes Meteorological Station in 2020. (Data derived from <http://aszalymonitoring.vizugy.hu>).

were not used, crops were harvested late, the seeds dried naturally. The average sunflower yield data was 4000 kg/ha from 20 parcels. First, crop yield data is filtered, removing incorrect values recorded by the yield monitor [30]. Commercial yield monitors are prone to erroneous data when harvested rows overlap, suggesting that there is a low yielding crop in specific areas of the field. Therefore, straight-line sequences of points that showed near-zero yield were removed from the

dataset. Calibrated and filtered crop yield data for this research were collected from the company that owns and manage the study site’s farming operation. Only yield data with the same width and distance were left corresponding to the combine header dimension (i.e., 2 × 6 m). We then converted the crop yield data to raster format using the IDW interpolation method in QGIS v.3.16 with 10 × 10 m same pixel size than satellite image. We used this data further as a response variable for

the crop yield estimation model using Sentinel-2 spectral reflectance.

### 2.2.2. Remote sensing data

We downloaded six cloud-free satellite images of the Sentinel-2 from the Copernicus Open Access Hub website (<https://scihub.copernicus.eu/dhus/#/home> accessed on 1 September 2019) [31] during the sunflower growing period from April to September, 2020. We downloaded all images in L2A format, bottom of atmosphere reflectance—meaning they had already been atmospherically and geometrically corrected. Sentinel-2 twin satellites (A and B) carry multispectral instruments (MSI) on board, offering 13 spectral bands at different spatial resolutions (10, 20, 60 m), which provides new opportunities for both regional and global agricultural monitoring [32]. The yield forecasting stage contains several steps. In Fig. 3 we summarize the overall research workflow. First, we resampled all images from different pixel sizes into 10 m resolution using the Sentinel applications platform (SNAP) version 8.0 (<https://step.esa.int> accessed on 1 September) [33] developed by ESA. We further extracted the study fields by mask layer using the official crop plan map shaped as a mask layer. Thereafter we created a grid rectangle (polygon) at  $10 \times 10$  m to extract pixel values for model development corresponding to the Sentinel-2 image spatial resolution. We extracted pixel values from 10 spectral bands (bands 2, 3, 4, 5, 6, 7, 8, 8A, 11 and 12) of Sentinel-2 using the point sampling tool—a free and open-source plugin in QGIS. Obtained spectral reflectance values were used as predictor variables in the regression analysis.

### 2.2.3. Selection of training and validation data set

The total of 20 sunflower fields were used in this study (Fig. 1). We used 10 sunflower fields for training model development and 10 fields for validation of the model. There were fields of different sizes thus selection of the training and validation data sets were made according to the size of the fields (Fig. 4). Every first parcel was selected as a training site and every second left out for the validation step to ensure similarity for both datasets.

### 2.3. Building yield estimation models and validation

RFR is based on the decision tree algorithm that was used to accomplish crop yield estimation [34]. RFR is a supervised machine learning technique that uses the ensemble learning method for regression. The main advantage of this method compared to the decision tree is the performance of RFR combines predictions from multiple machine learning algorithms to make a more accurate prediction than a single model [35]. The results acquired from each tree are based on a majority vote of all associated trees. Another advantage of RF over any other technique is it performs well on large datasets. A random forest regression model was implemented using the ‘randomForest’ package in R software (Liaw et al. [36]). Two parameters were adjusted to optimize the RF regression model: *ntree*, the number of trees grown in the regression forest, was set at 500; *mtry*, the number of different predictors sampled at each node (default = the number of predictors divided by 3). We created 6 models from six different months (April to September) using spectral bands as predictive variables to find the best correlation coefficient to predict crop yield. We based our yield estimation model on time series of Sentinel-2 (April to September) against crop reported statistics using RFR. First, we calculated average crop yield data for each pixel corresponding to the spatial resolution of Sentinel-2. Furthermore, we extracted the spectral reflectance of the 10 spectral bands. The best RFR model was obtained, and we tested and validated it in 10 different sunflower parcels. The result of the prediction from test sites was compared with observed yield data and residuals are calculated. To assess the performance of the prediction model accuracy, we calculated metrics including coefficient of determination ( $R^2$ ), and root means square error (RMSE) based on the following formulas:

$$R^2 = 1 - \frac{RSS}{TSS} \quad (1)$$

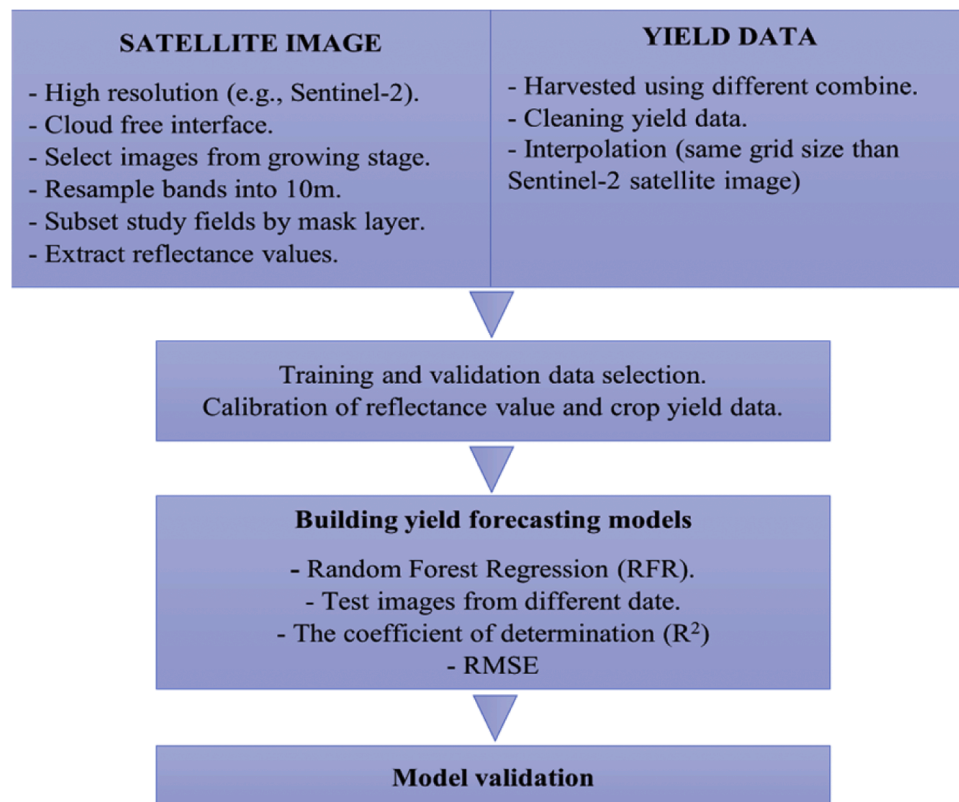


Fig. 3. The overall methodology adopted in this research.

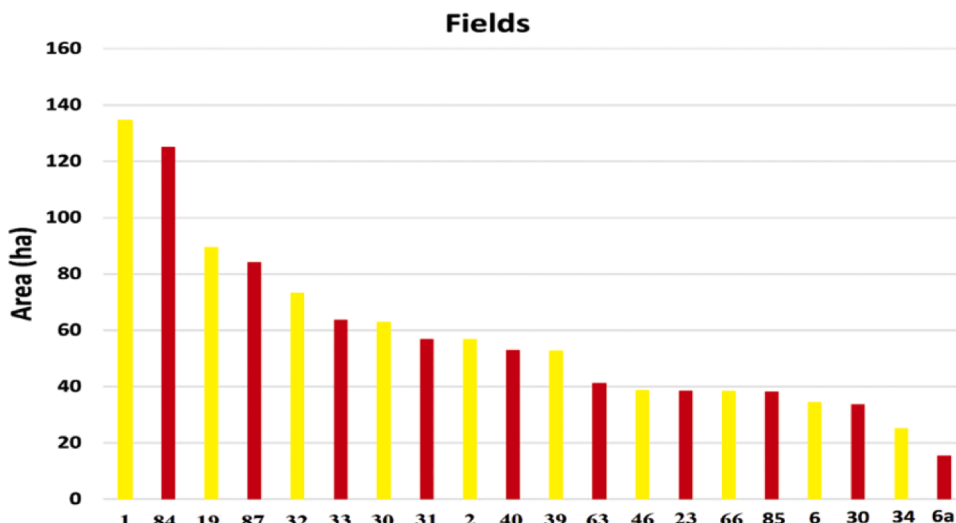


Fig. 4. Selection of training (yellow) and validation (red) sites according to field size.

$$RMSE = \sqrt{\frac{\sum_{i=1}^n (y_i - \hat{y}_i)^2}{n}} \quad (2)$$

### 3. Results

#### 3.1. Accuracy of RF regression model

We created six models using Sentinel-2 satellite images (April to September) that were captured during the growing period of sunflower (Fig. 5). We obtained a high coefficient of determination ( $R^2 = 0.84$ )

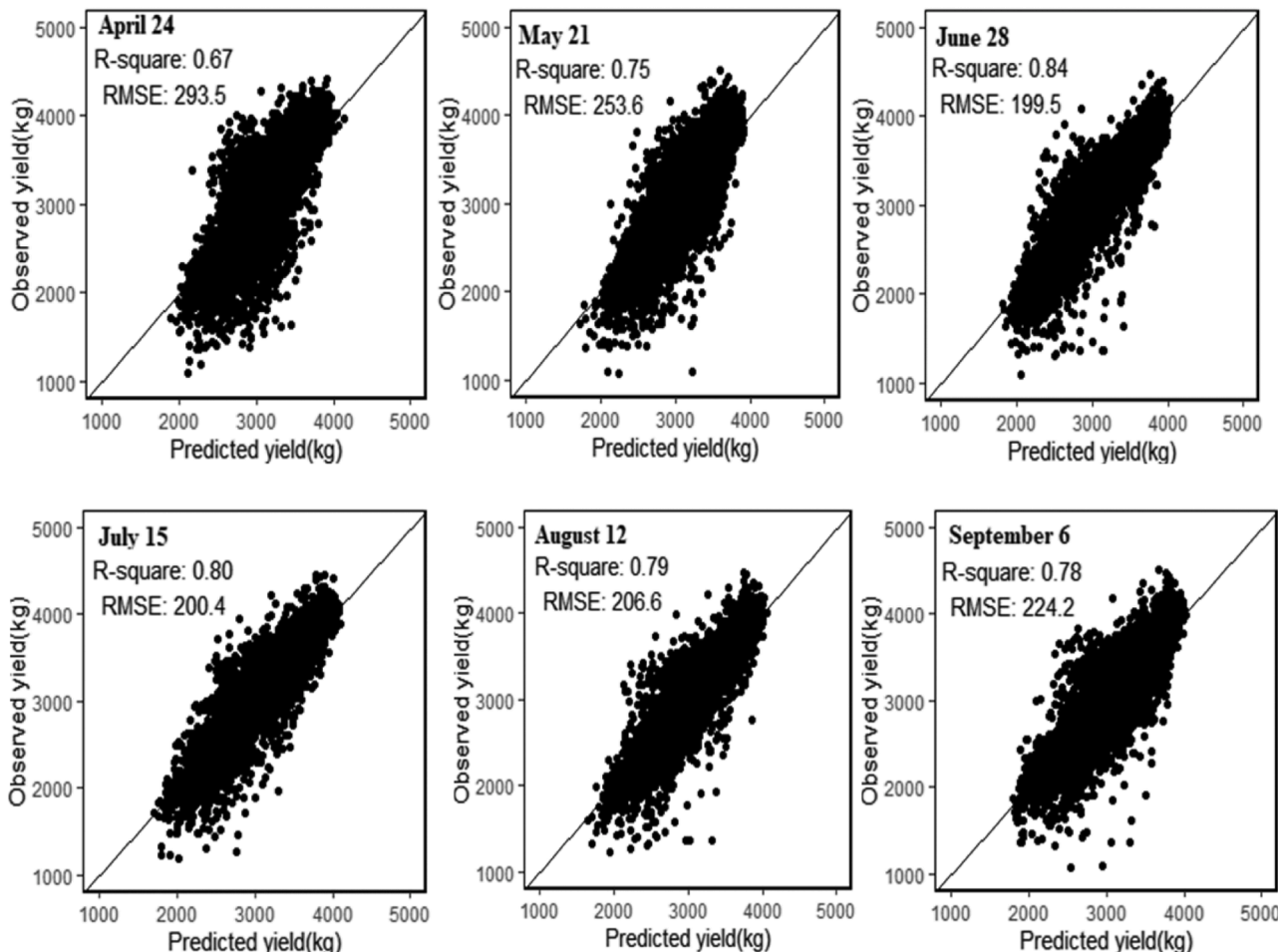


Fig. 5. Relationship between observed and estimated sunflower yield using RFR model of training data set.

between the training data sets for an image acquired on June 28 from the RFR model. In this study, Sentinel-2 10 spectral bands were used to build an RFR model based on crop yield data. The phenological stage showed that the sunflower was at its peak vegetative period at the end of June (Fig. 6). We observed the strongest coefficient of determination ( $R^2$ ) between 10 spectral bands and crop yield in June because it represented the highest vegetative period and the lowest relationship from April to May. The calibrated model was then validated on a completely independent data set that had a total of 10 fields for the 2020 seasons. A random forest regression model derived from RFR best model was used for further prediction of sunflower crop yield in test fields. The results showed that the high accuracy in the training data set did always represent high accuracy in the test data set.

### 3.2. Spatial prediction and validation

We created the crop yield spatial distribution map of the validation field for each pixel based on the best performing RFR model. For the validation, the satellite image captured on June 28 was used as it was found the best during training model development. Fig. 7 shows predicted sunflower yields for each pixel. Crop yield was very high where vegetation values were high, whereas the lowest crop yield came from the areas with low vegetation pixel values. We used the observed average sunflower crop yield from 10 parcels to validate the prediction model and to calculate the accuracy of the forecast. We compared the result of the predicted map with the observed crop yield provided by the combine harvester. Visually, the distribution map based on the regression models reflected the general pattern of the observed yield with a relatively small variation in the within-field patterns. From the predicted yield map, we were also able to highlight some areas underestimated and overestimated by the model.

For further analysis of the comparison between actual and estimated spatial distribution maps, we created residual maps (Fig. 8). In general, the residual map resembles the spatial distribution of the actual crop yield derived from the combine harvester, with some features on the underestimated and overestimated pattern from the estimated crop yield values highlighted. As we show in the residual map (Fig. 8), in Fields 23, 40, 63 and 84, the regression models showed slightly underestimated patterns across the fields. On the other hand, in Fields 30, 31 and 33, almost one-thirds of the area of the field had a tendency of overestimation, while small areas in the fields had a tendency to underestimate. These errors might be due to various reasons including elevation, different cultivars, inland excess water, and different agricultural management practices. The regression model was estimated slightly well across the fields such as 6, 85, and 87 with fewer errors. The field-

specific RMSE values showed that the accuracy of the models was different from field to field, as the RMSE values ranged between 121.9 and 284.5 kg/ha (Fig. 9).

## 4. Discussion

### 4.1. Factors affecting the accuracy of the regression models

Our results indicate that sunflower crop yield can be estimated using Sentinel-2 imagery with acceptable accuracy. Data distribution differences between each observation field used in the training and test data set might have caused the different output accuracy of the models. Different agronomic practices were performed within each observation field this might lead decrease in the accuracy of the model. Another factor that can affect the accuracy of the regression models is crop yield data which was taken from company. We do not know the calibration of the crop yield provided by the combine tractor thus we only used points with the same width and distance according to the combine header.

### 4.2. Crop yield distribution map and future development

The accuracy of the RFR model (RMSE 121.9 kg/ha) was more robust compared to a previous study by [25], who also predicted sunflower crop yield by assimilating leaf area index into a crop model (RMSE 7.49 q·ha<sup>-1</sup>). Our study demonstrated robust methods to predict the sunflower crop yield at the field scale based on Sentinel-2 satellite imagery and the observed yield data obtained from the combine harvester. To find the best period for estimating potential yield, we examined the daily spectral reflectance data produced by a time-series interpolation process for each Sentinel-2 pixel against yield maps recorded by the harvester machine. We used the determination of satellite-derived parameters in the crop modelling process. The sunflower is planted in the mid Spring, usually during April in Europe; seedlings emerge shortly thereafter, and tillering is completed during March. The validation of the RFR derived models produced good results in predicting sunflower yield. In addition, we obtained a better prognosis estimating the average sunflower yield for the most sensitive period (June and July) than that obtained using estimation models obtained individually from Sentinel-2 imagery on a particular day of the month. In summary, high spatial resolution remote sensing images such as Sentinel-2 images have significant potential in sunflower yield prediction. The crop yield distribution map can provide a better understanding of identifying areas with low or high yield for better management practices. The distribution map derived from the RFR model (Fig. 7) clearly shows the within-field and between-field patterns of crop yield spatial variability. Further research will focus on

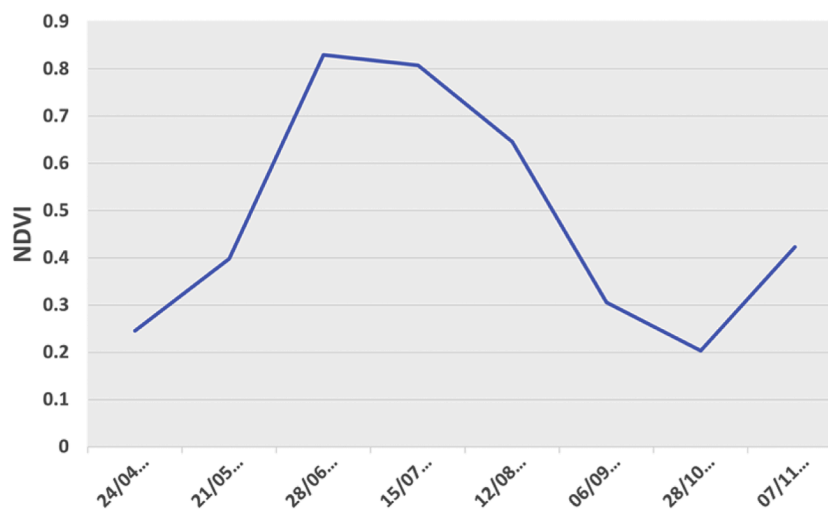


Fig. 6. Seasonal fluctuation of Sentinel-2 vegetation index (NDVI) in study parcel. Data are mean values from eight months.

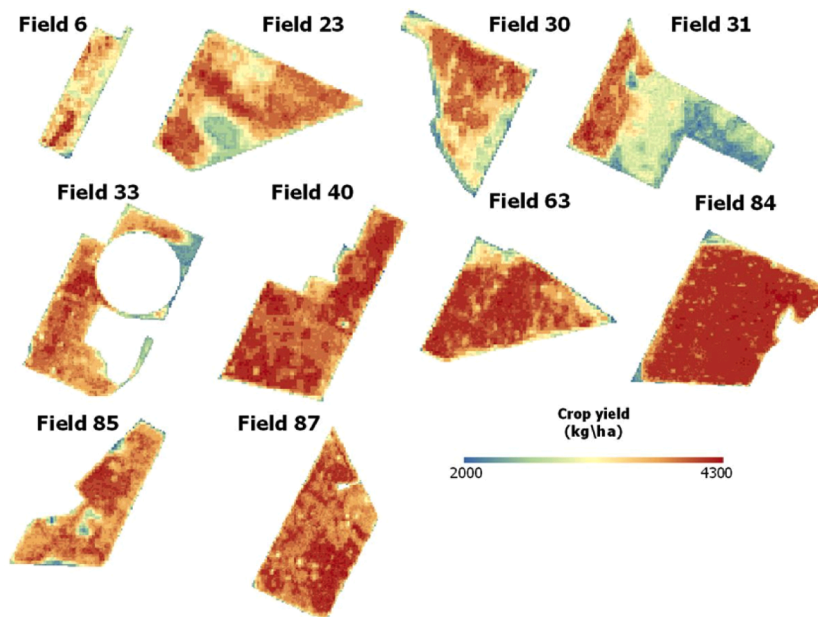


Fig. 7. Applying the field-scale yield model to pixels within each field in test sites.

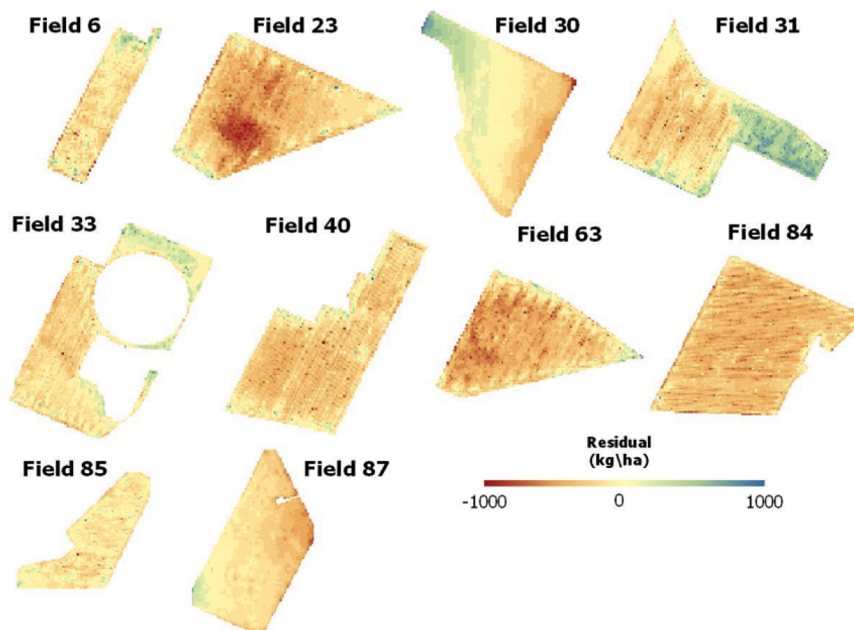


Fig. 8. Residual maps. Differences between observed and predicted sunflower crop yield.

the optimization of the proposed methodology through the incorporation of additional fields with different soil nutrient content, climate data with different crop species such as autumn wheat and hybrid corn, under different management and practices or in different areas and cultivation years. Our approach can therefore be enhanced by modifying it using deep learning or multivariable regression methods and hyperspectral data because it performs better than optical spectral reflectance methods in crop yield prediction and can enhance the result of the model [37–40].

### 5. Conclusions

This study demonstrates that the satellite-based RFR model successfully can predict sunflower crop yield at a pixel or field level. The

main purpose of our study was to develop a robust model for the estimation/prediction of sunflower yield at the field level using the spectral reflectance generated from Sentinel-2 satellite imagery. We derived our sunflower yield forecasting model based on 10 multi-spectral bands of Sentinel-2 remote sensing data. From techniques we developed based on six different months selected from the growing phase of the sunflower (April to September 2020), we determined that crop yield can be predicted 3–4 months before the harvesting stage. We found the highest relationship between Sentinel-2 spectral reflectance and crop yield data provided by the combine harvester on June 28 when the sunflower was 85–105 d into the flowering stage. The regression analysis using RFR was capable of predicting the crop yield of test fields with RMSE values ranging from 121.9 and 284.5 kg/ha. The satellite-based prediction model might be able to provide farmers with useful information about

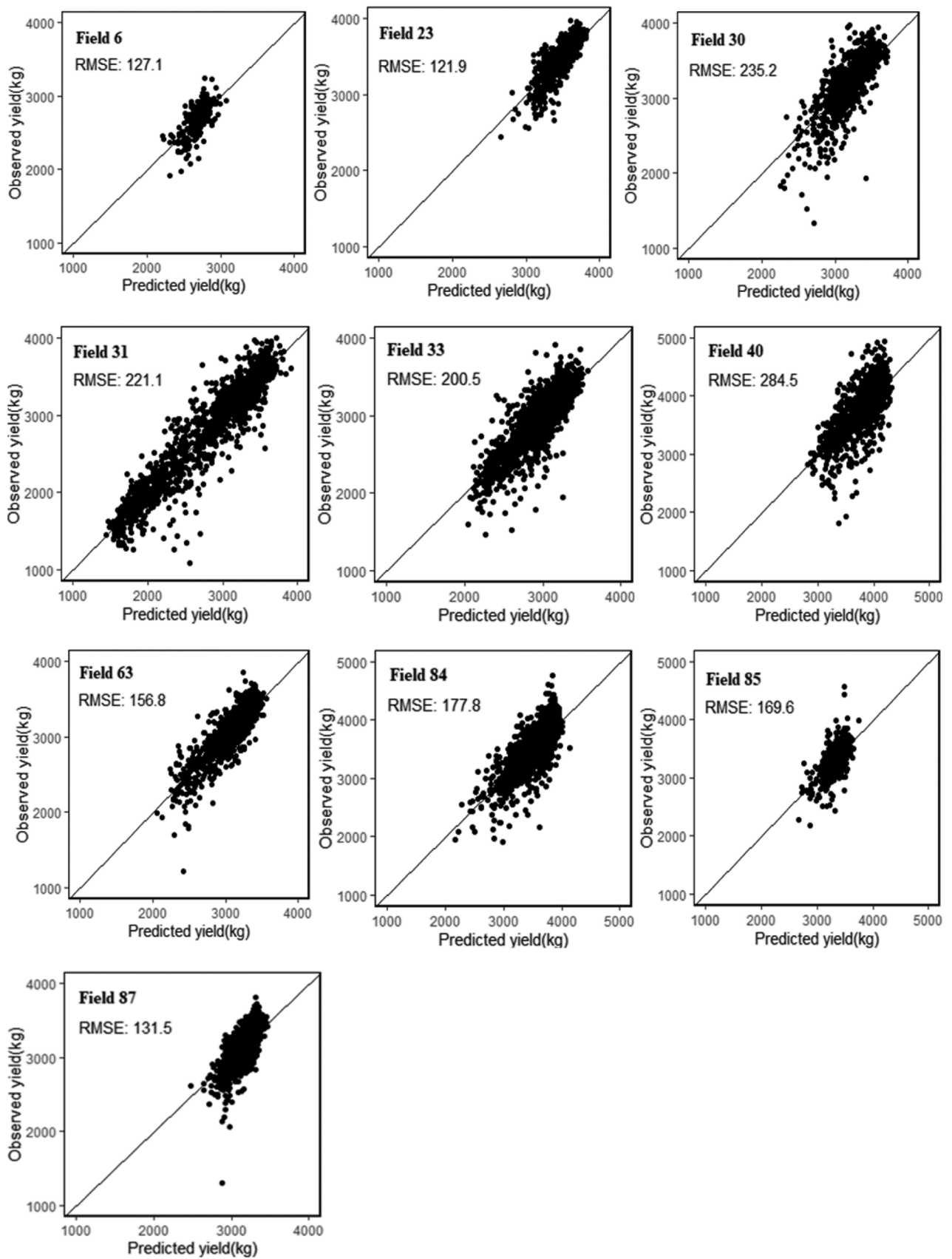


Fig. 9. RMSE values for individual fields using RFR model of the test data set.

field-specific variability in crop yield. With this proposed prediction model, it will be possible to forecast sunflower crop yield at the pixel or field level—which is of great interest to farmers, stakeholders, and decision-makers to prevent potential crop yield loss. The main advantage of our model lies in its simplicity and enhanced precision. Spectral reflectance derived from Sentinel-2 can accurately predict crop yields and could be implemented on a large or small scale. Prior knowledge of crop type, together with many known yields with images, will render predictions even more accurate. To the best of our knowledge, this is the crucial case study establishing a satellite-based estimation model for sunflower crop yield. This model is good for further application of crop yield prediction at the pixel and field level. The proposed method in this study is expected to be adapted for other locations and different crops by arranging a suitable training process.

### Data availability statement

The Sentinel-2 satellite images can be downloaded from the Copernicus Scientific Data Hub (<https://scihub.copernicus.eu/>). The sunflower yield data and R code are available from the corresponding author [Khilola Amankulova], upon reasonable request.

### CRediT authorship contribution statement

**Khilola Amankulova:** Conceptualization, Methodology, Project administration, Software, Formal analysis, Investigation, Data curation, Writing – original draft, Writing – review & editing, Visualization. **Nizom Farmonov:** Conceptualization, Methodology, Formal analysis, Resources, Investigation, Writing – review & editing. **László Muksi:** Conceptualization, Writing – review & editing, Supervision.

### Declaration of Competing Interest

The authors declare that they have no known competing financial interests or personal relationships that could have appeared to influence the work reported in this paper.

### Acknowledgements

Many thanks to Krisztián Bónus, Director of Precision farming and Commodity Plant Division, Nemzeti Ménesbirtok és Tangazdaság Zrt., Mezőhegyes who provided us with field data and allowed us to work in their fields.

### References

- [1] V. Mishra, J.F. Cruise, J.R. Mecikalski, Assimilation of coupled microwave/thermal infrared soil moisture profiles into a crop model for robust maize yield estimates over Southeast United States, *Eur. J. Agron.* 123 (2021), 126208, <https://doi.org/10.1016/j.eja.2020.126208>.
- [2] W.G.M. Bastiaanssen, S. Ali, A new crop yield forecasting model based on satellite measurements applied across the Indus Basin, Pakistan, *Agric. Ecosyst. Environ.* 94 (2003) 321–340, [https://doi.org/10.1016/S0167-8809\(02\)00034-8](https://doi.org/10.1016/S0167-8809(02)00034-8).
- [3] BS Adeleke, OO. Babalola, Oilseed crop sunflower (*Helianthus annuus*) as a source of food: Nutritional and health benefits, in: 8, 2020, pp. 4666–4684, <https://doi.org/10.1002/fsn3.1783>. Jul 31 PMID: 32994929; PMID: PMC7500752.
- [4] FAO. 2019 Food outlook - biannual report on global food markets. Rome. ISBN 978-92-5-131448-7.
- [5] S. Konyali, Sunflower production and agricultural policies in Turkey, *Soc. Sci. Res. J.* 6 (4) (2017) 11–19.
- [6] R.P. Sishodia, R.L. Ray, S.K. Singh, Applications of remote sensing in precision agriculture: a review, *Remote Sens.* 12 (2020) 3136, <https://doi.org/10.3390/rs12193136>.
- [7] P.J.A. Kleinman, A.N. Sharpley, R.W. McDowell, D.N. Flaten, A.R. Buda, L. Tao, L. Bergstrom, Q. Zhu, Managing agricultural phosphorus for water quality protection: principles for progress, *Plant Soil* 349 (2011) 169–182, <https://doi.org/10.1007/s11104-011-0832-9>.
- [8] L.F. Konikow, Long-term groundwater depletion in the United States, *Groundwater* 53 (2015) 2–9, <https://doi.org/10.1111/gwat.12306>.
- [9] F. Wen, Evaluation of the impact of groundwater irrigation on streamflow in Nebraska, *J. Hydrol.* v 327 (2006) 603–617, <https://doi.org/10.1016/j.jhydrol.2005.12.016>.
- [10] L. Leroux, M. Castets, C. Baron, M.-J. Escorihuela, A. Bégue, D. Lo Seen, Maize yield estimation in West Africa from crop process-induced combinations of multi-domain remote sensing indices, *Eur. J. Agron.* 108 (2019) 11–26, <https://doi.org/10.1016/j.eja.2019.04.007>.
- [11] J.A. Delgado, N.M. Short, D.P. Roberts, B. Vandenberg, Big data analysis for sustainable agriculture on a geospatial cloud framework, *Front. Sustain. Food Syst.* 3 (54) (2019), <https://doi.org/10.3389/fsufs.2019.00054>.
- [12] O. Elijah, T.A. Rahman, I. Orikumhi, C.Y. Leow, M.H.D.N. Hindia, An overview of Internet of Things (IoT) and data analytics in agriculture: benefits and challenges, *IEEE Internet Things J.* 5 (2018) 3758–3773, <https://doi.org/10.1109/JIOT.2018.2844296>.
- [13] K. Jha, A. Doshi, P. Patel, M. Shah, A comprehensive review on automation in agriculture using artificial intelligence, *Artif. Intell. Agric.* 2 (2019) 1–12, <https://doi.org/10.1016/j.iaia.2019.05.004>.
- [14] A.D. Boursianis, M.S. Papadopoulou, P. Diamantoulakis, A. Liopa-Tsakalidi, P. Barouchas, G. Salahas, K. Karagiannidis, S. Wan, S.K. Goudos, Internet of Things (IoT) and Agricultural Unmanned Aerial Vehicles (UAVs) in smart farming: a comprehensive review, in: , 2020, 100187, <https://doi.org/10.1016/j.iot.2020.100187>.
- [15] B. Koch, R. Khosla, W.M. Frasier, D.G. Westfall, D. Inman, Economic feasibility of variable-rate nitrogen application utilizing site-specific management zones, *Agron. J* 96 (2004) 1572–1580, <https://doi.org/10.2134/agronj2004.1572>.
- [16] Taylor, J.C.; Wood, G.A.; Thomas, G. Mapping yield potential with remote sensing. In Proceedings of the First European Conference on Precision Agriculture, London, UK, 7–10 September 1997; pp. 713–720.
- [17] A.A. Gitelson, Remote sensing estimation of crop biophysical characteristics at various scales, in: P.S. Thenkabail, J.G. Lyon, A. Huete (Eds.), *Hyperspectral Remote Sensing of Vegetation*, CRC Press, Boca Raton, FL, USA, 2012, pp. 329–354. Eds.
- [18] Z. Ji, Y. Pan, X. Zhu, J. Wang, Q. Li, Prediction of crop yield using phenological information extracted from remote sensing vegetation index, *Sensors* 21 (2021) 1406, <https://doi.org/10.3390/s21041406>.
- [19] C. Funk, M.E. Budde, Phenologically-tuned MODIS NDVI-based production anomaly estimates for Zimbabwe, *Remote Sens. Environ.* 113 (2009) 115–125, <https://doi.org/10.1016/j.rse.2008.08.015>.
- [20] D. Goffart, Y. Cornet, V. Planchon, J.P. Goffart, P. Defourny, Field-scale assessment of Belgian winter cover crops biomass based on Sentinel-2 data, *Eur. J. Agron.* 126 (2021), 126278, <https://doi.org/10.1016/j.eja.2021.126278>.
- [21] F.N. Adrianasolo, P. Casadebaig, E. Maza, L. Champolivier, P. Maury, P. Debaeke, Prediction of sunflower grain oil concentration as a function of variety, crop management and environment using statistical models, *Eur. J. Agron.* 54 (2014) 84–96, <https://doi.org/10.1016/j.eja.2013.12.002>.
- [22] C. Cavalariis, S. Megoudi, M. Maxouri, K. Anatolitis, M. Sifakis, E. Levizou, A. Kyriarissis, Modeling of durum wheat yield based on Sentinel-2 imagery, *Agronomy* 11 (2021) 1486, <https://doi.org/10.3390/agronomy11081486>.
- [23] A. Nagy, A. Szabó, O.D. Adeniyi, J. Tamás, Wheat yield forecasting for the Tisza river catchment using landsat 8 NDVI and SAVI time series and reported crop statistics, *Agronomy* 11 (652) (2021), <https://doi.org/10.3390/agronomy11040652>.
- [24] R.A. Schwalbert, T. Amado, G. Corassa, L.P. Pott, P.V.V. Prasad, I.A. Ciampitti, Satellite-based soybean yield forecast: integrating machine learning and weather data for improving crop yield prediction in southern Brazil, *Agric. For. Meteorol.* 284 (2020), 107886, <https://doi.org/10.1016/j.agrformet.2019.107886>.
- [25] R. Trépos, L. Champolivier, J.-F. Dejoux, A. Al Bitar, P. Casadebaig, P. Debaeke, Forecasting sunflower grain yield by assimilating leaf area index into a crop model, *Remote Sens.* 12 (2020) 3816, <https://doi.org/10.3390/rs12223816>.
- [26] M. Wang, F. Tao, W. Shi, Corn yield forecasting in northeast China using remotely sensed spectral indices and crop phenology metrics, *J. Integr. Agric.* 13 (2014) 1538–1545, [https://doi.org/10.1016/S2095-3119\(14\)60817-0](https://doi.org/10.1016/S2095-3119(14)60817-0).
- [27] O.G. Narin, S. Abdikan, Monitoring of phenological stage and yield estimation of sunflower plant using Sentinel-2 satellite images, *Geocarto. Int.* 32 (2022) 1378–1392, <https://doi.org/10.1080/10106049.2020.1765886>.
- [28] R. Fieuzal, C. Marais Sicre, F. Baup, Estimation of sunflower yield using a simplified agrometeorological model controlled by optical and SAR satellite data, *IEEE J. Sel. Top. Appl. Earth Obs. Remote Sens.* 10 (2017) 5412–5422, <https://doi.org/10.1109/JSTARS.2017.2737656>.
- [29] K. Amankulova, N. Farmonov, A. Gudmann, K. Bónus, L. Muksi, Investigation of the reason of affected hybrid corn in agricultural fields by using multi-temporal Sentinel-2 images in Mezőhegyes, in: South-Eastern Hungary. GIS Conference and Exhibition the Meeting of Theory and Practice in GIS, University of Debrecen, Hungary, 2021, pp. 25–34, 11–12 November.
- [30] T.P. Kharel, A. Maresma, K.J. Czymmek, E.K. Oware, Q.M. Ketterings, Combining spatial and temporal corn silage yield variability for management zone development, *Agron. J.* 111 (2019) 2703–2711, <https://doi.org/10.2134/agronj2019.02.0079>.
- [31] Open Access Hub. Available online: <https://scihub.copernicus.eu/> (accessed on 1 September 2019).
- [32] D. Vijayasekaran, SEN2-AGRI – CROP type mapping pilot study using sentinel-2 satellite imagery in India, *Int. Arch. Photogramm. Remote Sens. Spatial Inf. Sci.* (2019) 175–180, <https://doi.org/10.5194/isprs-archives-XLII-3-W6-175-2019-XLII-3-W6>.
- [33] European Space Agency. STEP—science toolbox exploitation platform. Available online: <http://step.esa.int> (accessed on 1 September 2019).
- [34] P.F. Smith, S. Ganesh, P. Liu, A comparison of random forest regression and multiple linear regression for prediction in neuroscience, *J. Neurosci. Methods* 220 (2013) 85–91, <https://doi.org/10.1016/j.jneumeth.2013.08.024>.

- [35] K. Fawagreh, M.M. Gaber, E. Elyan, Random forests: from early developments to recent advancements, *Syst. Sci. Control Eng.* 2 (2014) 602–609, <https://doi.org/10.1080/21642583.2014.956265>.
- [36] Liaw, A.; Wiener, M.; Breimann, L.; Cutler, A. Randomforest: breiman and Cutler's random forests for classification and regression. 2018. Available online: <https://cran.r-project.org/web/packages/randomForest/randomForest.pdf> (accessed on 15 January 2021).
- [37] B. Csendes, L. Mucsi, Identification and spectral evaluation of agricultural crops on hyperspectral airborne data, *J. Environ. Geogr.* 9 (2016) 49–53, <https://doi.org/10.1515/jengeo-2016-0012>.
- [38] J.P. Ferrio, D. Villegas, J. Zarco, N. Aparicio, J.L. Araus, C. Royo, Assessment of durum wheat yield using visible and near-infrared reflectance spectra of canopies, *Field Crops. Res.* 94 (2005) 126–148, <https://doi.org/10.1016/j.fcr.2004.12.002>.
- [39] M.U. Liaqat, M.J.M. Cheema, W. Huang, T. Mahmood, M. Zaman, M.M. Khan, Evaluation of MODIS and Landsat multiband vegetation indices used for wheat yield estimation in irrigated Indus Basin, *Comput. Electron. Agric.* 138 (2017) 39–47, <https://doi.org/10.1016/j.compag.2017.04.006>.
- [40] X. Ye, K. Sakai, M. Manago, S. Asada, A. Sasao, Prediction of citrus yield from airborne hyperspectral imagery, *Precis. Agric.* 8 (2007) 111–125, <https://doi.org/10.1007/s11119-007-9032-2>.